Proceedings of the 6th International Conference on the Application of Physical Modelling in Coastal and Port Engineering and Science (Coastlab16)

Ottawa, Canada, May 10-13, 2016

SURFACE TURBULENCE ON BORES AND SURGES PROPAGATING ON SMOOTH AND ROUGH BEDS

D. WÜTHRICH[1], M. PFISTER[1], P. MANSO[1], G. CONSTANTINESCU[2], A.J. SCHLEISS[1]

[1] *Laboratoire de Constructions Hydrauliques (LCH) – Ecole Polytechnique Fédérale de Lausanne (EPFL), Switzerland, davide.wuthrich@epfl.ch, michael.pfister@epfl.ch, pedro.manso@epfl.ch and anton.schleiss@epfl.ch*

[2] *Civil and Environmental Engineering – The University of Iowa, USA, sconstan@engineering.uiowa.edu*

ABSTRACT

Hydrodynamic waves are characterised by unsteady, highly turbulent and irregular behaviours. In nature, such phenomena can be observed in dam breaks, impulse waves and tsunamis. Both wet bed bores and dry bed surges were experimentally reproduced on smooth and rough surfaces. For all tested scenarios a front propagating in the channel was observed, with secondary waves with various frequencies occurring behind the propagating front. Such phenomena are probably a consequence of the non-hydrostatic pressure distribution around the bore front. The present study investigates in both time and frequency domains, the distribution of the frequencies observed on top of the bore. The latter represent the surface fluctuations of a bore behind the front. Measurements allowed to characterise the eddy-size distribution for all configurations. Results also showed that the most recurring frequencies are between 0.5 and 2 Hz. Furthermore, it was shown that the first part of the wave was characterised by high-amplitude oscillations associated with greater energy content.

KEYWORDS: Hydrodynamic Waves, Tsunami, Roughness, Surface Fluctuations, Spectral analysis

1 INTRODUCTION

Hydrodynamic waves are characterised by a sudden release of a large water volume, resulting into an unsteady, highly turbulent and irregular behaviour. In nature, such hydrodynamic waves correspond to Impulse waves and Tsunamis. "*Man-made*" dam-break waves have a similar behaviour, and their advanced physical and mathematical developments are widely used to describe and characterise hydrodynamic waves. Various experimental set-ups are used to generate bores, including wave pistons (Ramsden 1993 and Wilson et al. 2009), dam breaks (Cross 1697, Yeh 1989, Arnason et al. 2009 and Nistor et al. 2009) and vertical release (Chanson et al. 2002, Meile 2007, Rossetto et al. 2011 and Wüthrich et al. 2016). Regardless of the technique used, a propagating front is observed. Thereafter, secondary waves with various frequencies occur behind the bore front. For unbroken cases such phenomena might be classified as Favre secondary waves (Favre 1935, Henderson 1966). The behaviour of secondary oscillations was previously investigated for dam break waves (Marche et al. 1995) and for open channel flows (Meile et al. 2013, Terrier et al. 2014). Their appearance is probably due to the non- hydrostatic pressure distribution around the wave front (Soares-Frazao and Zech 2002). A theory implying the superposition of wavelets with different velocities was developed by Chow (1959). Some specific studies focusing on turbulence in bores were carried out by Yeh and Mok (1990) who compared their behavior to hydraulic jumps. A "*generation-advection cycle*" was observed, in which eddies were formed in the roller and then advected behind the front. For large Froude numbers, the whole bore was saturated with turbulence. The turbulent behaviour in terms Reynolds stresses and instantaneous velocities was addressed by Koch and Chanson (2009) for bores propagating on wet bed. The effect of roughness was analysed by Chanson (2010). Some comparison with actual tidal bores in the Garonne River (France) was presented by Reungoat et al. 2015.

The majority of the previous studies focused on the investigation of the turbulent bore front (Yeh and Mok 1990, Docherty and Chanson 2012, Leng and Chanson 2015). Nevertheless there is no comprehensive theoretical framework to describe the behaviour of bores and surges behind the water front, whose oscillating behavior was observed in various channel configurations and for different flow conditions. The purpose of this study is to further investigate the fluctuating behaviour of wet bed bores and dry bed surges behind the front. Both smooth and rough beds were considered and data were analysed in frequency and time domains. The results yielded a characterisation of the free-surface oscillations according to the time evolution of the bore. Significant differences between the structure of the oscillations in the near-front region and in the region situated away from the front were observed. These differences were analyzed in terms of their spectral energy distribution.

2 EXPRIMENTAL SET UP AND ACQUISITION SYSTEM

Large-scale experiments were carried out at the Laboratory of Hydraulic Constructions (LCH) of EPFL, Switzerland. A vertical release technique was used with an upper reservoir of 7 m^3, linked to a lower basin through three independent pipes with identical internal diameter of 0.31 m. The experimental set up is presented in Figure 1. The discharge released was controlled using the number of pipes, producing bores and surges with different periods and amplitudes; the bores produced corresponded to an initial equivalent impoundment depth d_0 = 0.7 m for the classical dam-break scenario (Wüthrich et al. 2016). This technique was used to generate both wet bed bores and dry bed surges on smooth and rough beds. The wave propagation took place in a 14 m long and 1.4 m wide horizontal channel. The tests with a smooth bed took place on painted wooden panels with a Darcy-Weisbach friction factor measured to $f \approx 0.01$. To increase the roughness of the channel bed, an artificial green carpet was added; the latter had a thickness of 7 mm and some detailed steady state experiments were carried out to measure the friction factor $f \approx 0.04$, corresponding to an equivalent roughness k_s = 2.8 mm; this value is consistent with the findings of Choufi et al. (2014) for a similar material. The bore was characterised in terms of velocity and height using 7 Ultrasonic distance Sensors (US) installed along the channel (at x = 2, 10.1, 12.1, 13.1, 13.35, 13.6 and 13.85 m). An additional US sensor was installed in the upper reservoir to provide the initial time reference. The US sensors had a sampling frequency of 12.5 Hz and the analysis was carried out using a 6 Hz cut-off frequency, in accordance with Nyquist-Shannon theorem.

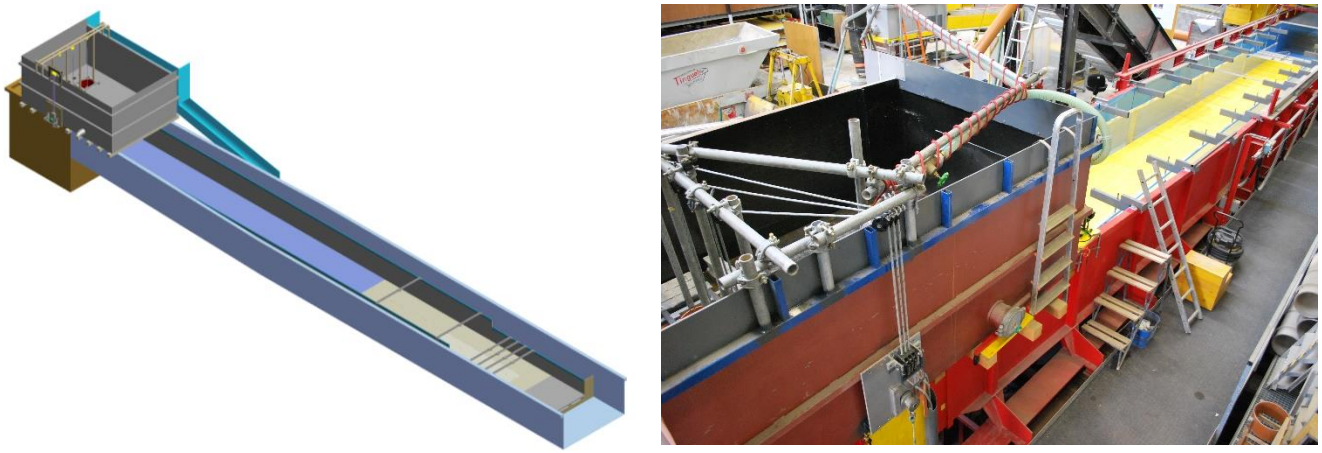

Figure 1. Pictures of the experimental set-up: (left) numerical and (right) physical model

3 VISUAL OBSERVATIONS

Tests on both smooth and rough bed were carried out over dry and wet conditions. For the present study four tests were selected. Details concerning the experiments can be found in Table 1. Overall, dry bed surges and wet bed bores had a different behaviour. Dry bed surges presented a thin front followed by a constant increase in water depth following the front and no major aeration was observed, whereas wet bed bores presented a highly turbulent, recirculating roller propagating over an irrotational, initially still, water level. According to Yeh and Mok (1990) the roller was formed by the flow separation initiated at the front toe resulting from the streamline divergence caused by the sudden raise in water depth. A similar phenomenon was observed by Leng and Chanson (2015) for tidal bores, positive surges and hydraulic jumps.

Wet bed bores showed a sudden increase in water height, followed by a relatively long and constant water height. For both wet bed bores and dry bed surges, less aeration was observed behind the front and some secondary waves with multiple time periods were recognised. The surface oscillation presented a 3-dimensional pattern and some movements were also observed in the transversal direction. Some model effects were observed at the beginning of the channel, however these disappeared during the propagation of the wave along the channel. Pictures of the propagating bores and surges are presented in Figure 2.

Table 1. Experimental tests performed for the present study

	Bed surface	Bed condition	Pipe number	Equivalent impoundment depth (d_0)
Wave 23	Smooth (f = 0.01)	Dry	3P	0.7
Wave 24	Smooth (f = 0.01)	Wet – 5 cm	3P	0.7
Wave 32	Rough (f = 0.04)	Dry	3P	0.7
Wave 34	Rough (f = 0.04)	Wet – 5 cm	3P	0.7

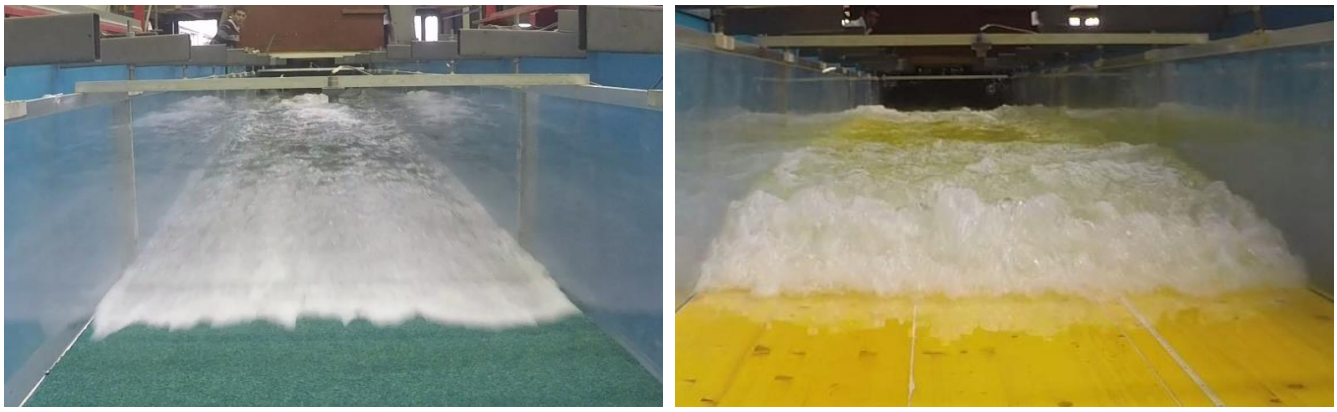

Figure 2. Propagating bores: (left) surge over rough bed, d_0 = 0.7 m, f = 0.04; (right) bore over wet bed, h_0 = 0.05 m, f = 0.01

4 BORE PROFILES AND SURFACE OSCILLATIONS

Detailed bore profiles were obtained at different locations along the channel. Results showed that at US7 (x = 13.85 m from channel inlet) the wave was fully developed for all scenarios. The time and space evolutions of the wave profiles are presented in Figure 3. The correspondence between time and space domains is obtained through an average wave front velocity ($x = U \cdot t$). Results clearly indicated that the surge propagating on the rough bed had lower velocities than the surge propagating on the smooth bed. The measurements confirmed the visual observations and the profiles showed that bores over a wet bed presented similar behaviours regardless of the bed roughness. The findings suggested that the still water level had more influence than the bed roughness. The profiles obtained for the dry bed surges showed a constantly increasing behaviour directly followed by the decreasing limb, whereas bores over wet bed presented a sudden raise followed by a relatively constant water level (*plateau*) before decreasing. These behaviours are in agreement with the theory of Ritter (1892) and Stoker (1952) for dam break waves on dry and wet bed respectively.

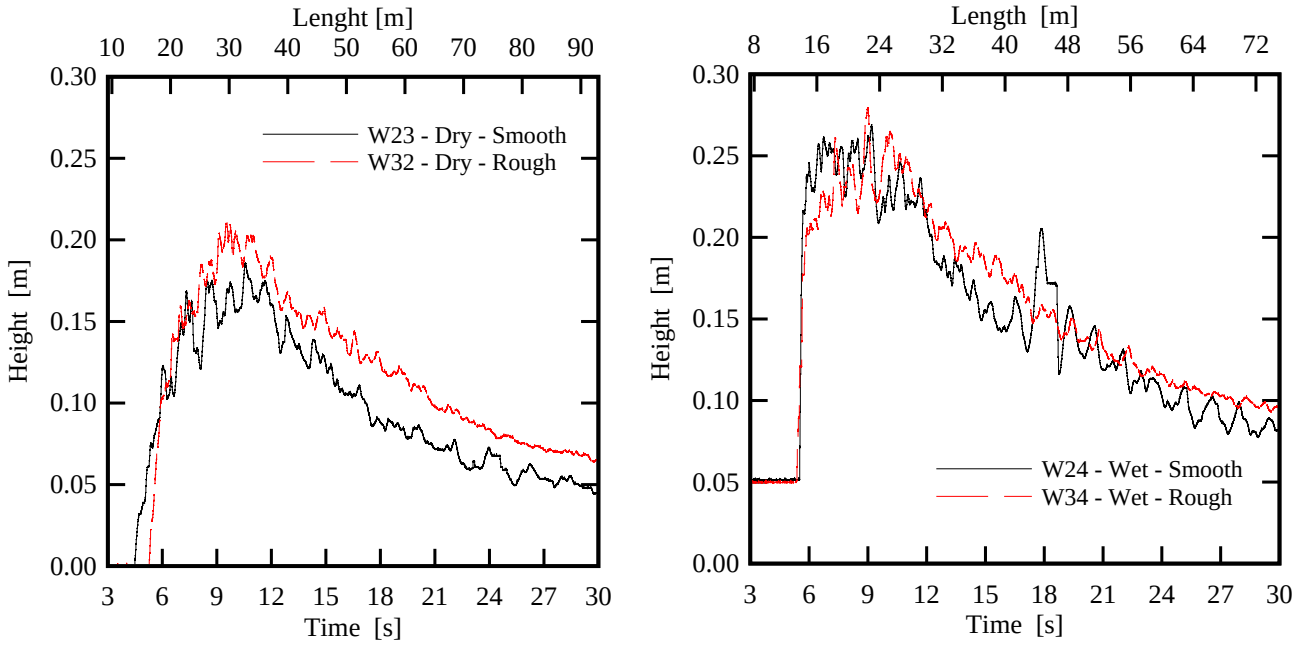

Figure 3. Comparison of wave behaviour on smooth and rough beds for: (left) dry bed surges; (right) wet bed bores for identical release conditions

Based on the bore front celerity (U), both the Reynolds (Re) and Froude (Fr) numbers of the flow were calculated using the expressions presents in Table 2, where D_H is the hydraulic diameter ($D_H = 4 \cdot R$), ν the kinematic viscosity of water, g the gravity constant and h the wave height. For the wet bed bore a bore Froude number (Fr_B)was also calculated based on the initial still water depth (h_0) (Yeh and Mok 1990, Leng and Chanson 2015). Results showed similar values of the flow Reynolds number for all configurations, with $Re = 2 \cdot 10^7$ during the wave peak. The relatively high values of the Reynolds number, computed using the front velocity and the maximum wave height (that might not occur at the same time) represent an upper

Table 2. Experimental tests performed for the present study

	U [m/s]	h_{max} [m]	$Re = \frac{U \cdot D_H}{\nu}$	$Fr = \frac{U}{\sqrt{g h_{max}}}$	$Fr_B = \frac{U}{\sqrt{g h_0}}$
Dry bed surge, smooth	3.55	0.185	$2.52 \cdot 10^7$	2.63	-
Dry bed surge, rough	2.86	0.220	$2.10 \cdot 10^7$	1.94	-
Wet bed bore, smooth	2.74	0.269	$2.12 \cdot 10^7$	1.68	3.91
Wet bed bore, rough	2.74	0.279	$2.15 \cdot 10^7$	1.66	3.92

value indicating a high level of turbulence inside the wave. The higher velocities of the dry-bed surges were compensated by the higher water elevation for the wet bed bores, explaining the similarity of the resulting values for all scenarios. For the dry bed surges, higher values of the Froude number were obtained. Similarly to some previous studies, a bore Froude number was calculated, showing that only strong and fully developed bores were considered. For all configurations a bore Froude number $Fr_B > 2$ was found, implying that the flow behind the bore front was saturated with advected eddies (Yeh and Mok 1990).

The US sensors also captured some secondary wave patterns behind the front and all tests presented multiple fluctuations of the water surface with frequencies varying from large to small scale. Some substantial differences were observed between the increasing and decreasing limbs of the wave, as the first seemed to have a higher density of secondary waves with greater amplitude and shorter periods. According to Yeh and Mok (1990) the fluctuations and the turbulent formations immediately behind the front are related to the behaviour of the propagating roller. Furthermore, a "*generation-advection cycle*" was observed, suggesting that the eddies formed inside the roller and were then advected in the flow, where a vertical stretch was detected. The secondary turbulence patches were related to the intermittent nature of the flow, as discussed by Longuet-Higgins and Turner (1974). A difference in water elevation between the smooth and the rough configurations was observed in the steady flow following the wave. For both surges and bores, the bores propagating over a rough bed was characterised by a lower level of surface turbulence with fewer fluctuations than those observed for the smooth bed cases. This might be attributed to the larger turbulence intensities of the flow generated over a rough bed, resulting in a more efficient dissipation of the eddies than on smooth bed, without interaction with the air-water interface. For the smooth-bed cases, the less efficient energy dissipation inside the flow would then result into enhanced surface turbulence with a repeating pattern to dissipate the remaining energy.

5 SPECTRUM ANALYSIS

To get an insight in the surface fluctuations of the waves, an exploratory spectral analysis was carried out using the transient water level data presented in Figure 3. First a Fourier Fast Transform (FFT) was applied to all raw height signals to identify the density of the frequencies observed on the water surface. The Fourier transform decomposes a signal into its frequency components. Results are presented in Figure 4 for all tests. As expected, a predominance of the low frequencies was observed for all profiles. Furthermore, some typical turbulent profiles associated with open channel flows were observed for both bores and surges.

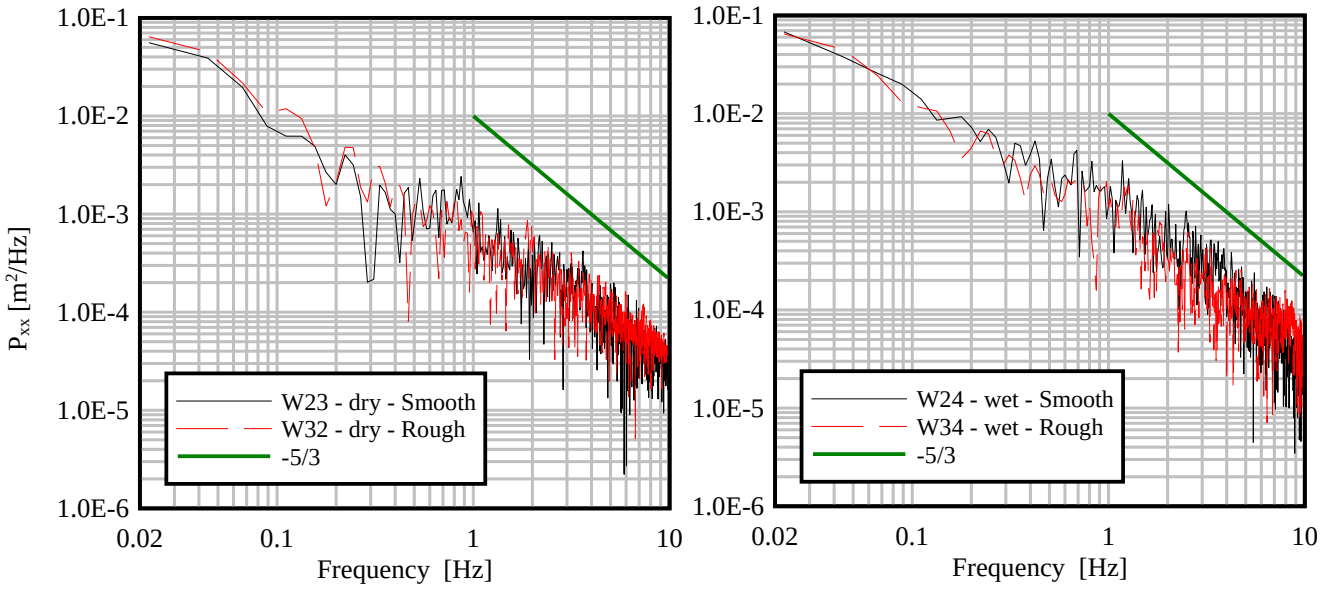

Figure 4. Spectral density functions for wave profile raw signals: (left) dry bed surges; (right) wet bed bores (acquisition frequency 12.5 Hz, duration of the raw signal around 30s each, Figure 3)

The high-frequency part of the spectrum followed the -5/3 decay law predicted by the Kolmogorov (1931) turbulent cascade theory, implying energy transfer from larger scales to lower scales all the way to viscous sub-layer. Although it is not supported by a solid theoretical explanation for bores and limited to the extent of the observed transient signals, is the authors' impression that the oscillation of the wave surface can give an insight of the eddy size distribution inside the wave, and therefore on the energy content of the secondary waves. A second analysis was carried out to characterise the surface turbulence, where the oscillations of the secondary waves were isolated using a "*Reynolds-like*" decomposition, in which a time-dependent moving average was subtracted from the original signal:

$$h'(t) = h(t) - h_{m.av}(t)$$

where $h'(t)$ is the fluctuation, $h(t)$ the original profile and $h_{m.av}(t)$ the moving average over a period of 3 seconds. This value was selected by the authors as it represented the shortest period that allowed to isolate the surface oscillations from the profile while keeping the fluctuating behaviour. The decomposition and the obtained signals are presented in Figure 5 for all scenarios. Given their substantial difference, the signal was then divided into two main parts, corresponding to the head and the tail of the main wave, each portion lasting around 10 seconds. The front was visually characterised by the presence of higher frequencies with a greater amplitude, whereas the tail part was characterised by lower amplitude oscillations with better regularity. Visually, this difference in signal is clearly presented in Figure 5. To improve the precision of the spectral analysis, several data sets from identical tests were summed up in order to obtain a longer signal for the FFT, hereafter called "ensemble signal". All the considered sub-sets had similar values in terms of their average and variance.

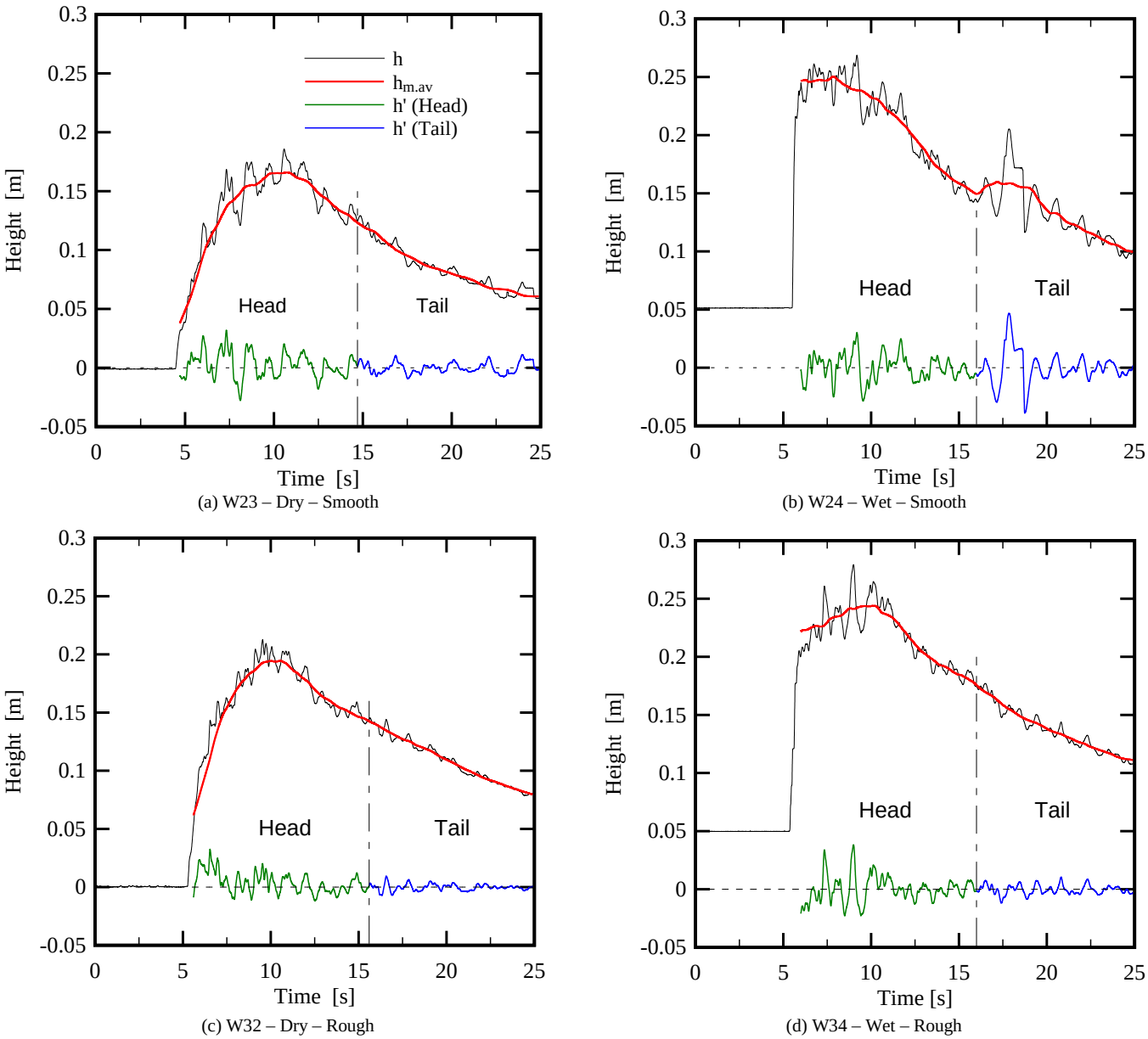

(a) W23 – Dry – Smooth

(b) W24 – Wet – Smooth

(c) W32 – Dry – Rough

(d) W34 – Wet – Rough

Figure 5. Decomposition of the original profile (h) in moving average ($h_{m.av}$) and fluctuations (h') for a single data-set

A Fourier Fast Transform (FFT) was applied to the ensemble signals (head and tail, smooth and rough); the results are presented in Figure 6 for all configurations. As observed for the raw signal (Figure 4), the spectra for the ensemble signals for all scenarios and for each part of the wave presented a typical profile similar to the previous ones, including the −5/3 slope for the Kolmogorov inertial sub-range (not shown). For this analysis the remaining lower frequencies were not considered, as they represented a residual of the moving average decomposition. For both dry bed surges and wet bed bores the highest density of frequencies were observed for $0.5 < F < 2$ Hz, corresponding to wave periods of 0.5 to 2 seconds. The energy content of frequencies above 2 Hz was small compared to that of the lower frequencies. For all configurations a lower density was observed in the tail part of the signal and overall higher peaks were recorded for waves propagating over smooth bed. For the tail part a dominant frequency is clearly observed for $F = 0.6$ Hz in the rough bed cases, corresponding to a wave period of 1.4 s. If an average velocity of 2.5 m/s is assumed a wavelength of 3.5 m is obtained, which is consistent with visual observations (Figure 2).

Overall, the spectra confirmed the visual observations that the tail part of the signal contained waves with longer periods compared to the head part. Especially in the tail, less smaller-scale turbulence was observed for the rough bed cases. For the head part, a single dominant frequency could not be recognised, however the signal was composed of multiple repeating ones, proving the high level of turbulence in the approaching wave.

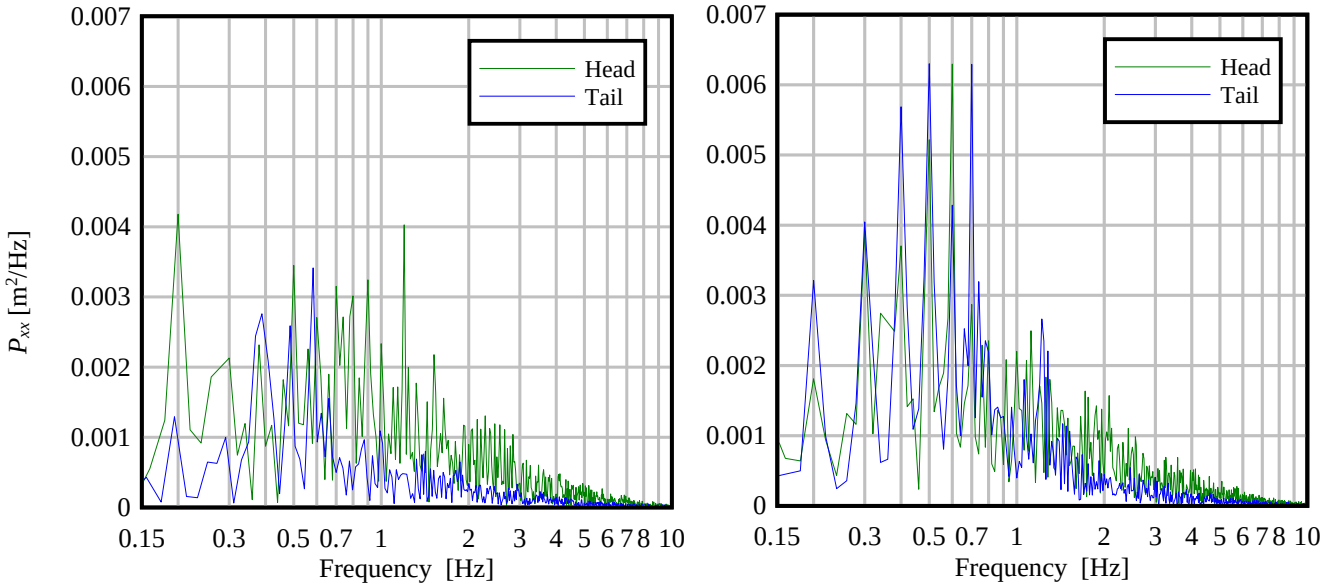

(a) Dry – Smooth (5 sub data-sets)

(b) Wet – Smooth (5 sub data-sets)

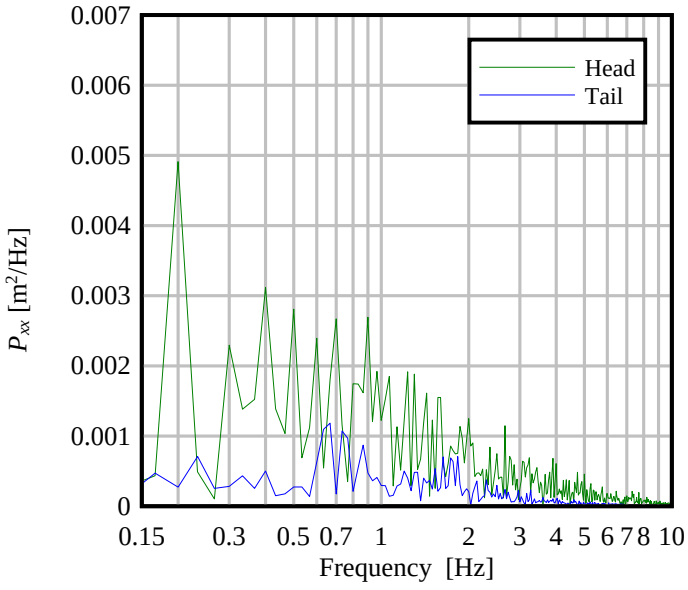

(c) Dry - Rough (3 sub data-sets)

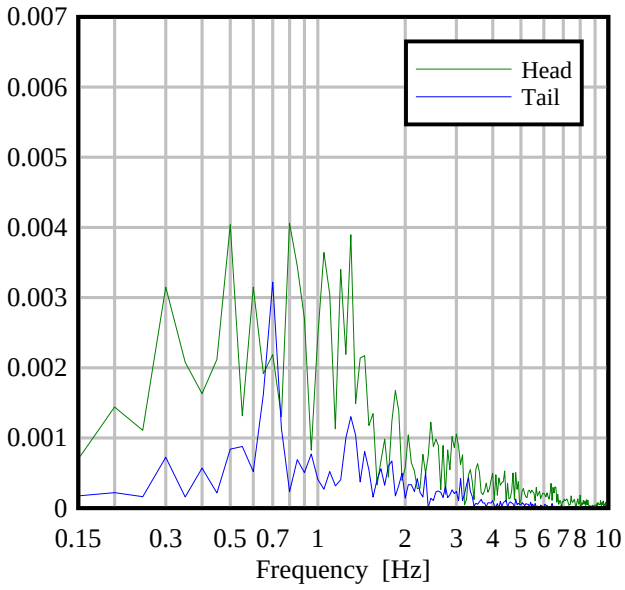

(d) Wet – Rough (2 sub data-sets)

Figure 6. Spectra obtained for the ensemble signals of the wave height fluctuations for both parts of the wave (head and tail) for all configurations

Table 3. Variance values for $0.5 < F < 6$ Hz for all tested configurations

	Dry, Smooth	Wet, Smooth	Dry, Rough	Wet, Rough
σ^2 [0.5-6 Hz] – Head	0.0031	0.0031	0.0030	0.0045
σ^2 [0.5-6 Hz] – Tail	0.0012	0.0022	0.0010	0.0015

The integral of the spectral density with frequencies between 0.5 and 6 Hz was computed for all configurations; the upper limit was chosen based on the Shannon-Nyquist Theorem. The integral corresponds to a fraction of the signal's variance or, in other words, to the energy associated with the mentioned frequency range; results are presented in Table 3. It was noted that for all configurations the head part of the wave had a higher energy content associated with frequencies in the interval $0.5 < F < 6$ Hz. For the tail signal, a higher energy content was obtained for the wet configurations, confirming the visual observation of a higher turbulent intensity inside the bore wake for such configurations.

6 CONCLUSIONS

Hydrodynamic waves such as dam break, impulse waves and tsunamis are highly unsteady flows characterised by a high level of turbulence and irregular surface oscillations. The aim of the present study was to gain a better understating of the secondary waves that are commonly observed behind wet bed bores and dry bed surges. The investigation of the surface oscillations allowed a better understanding of the internal turbulent behaviour and the eddy size distribution close to the top of the wave. The research was based on an experimental approach and a vertical release technique was used to produce both surges and bores on smooth and rough beds. The produced wet bed bores and dry bed surges propagated on a 14 m horizontal channel and were investigated in terms of height by means of 7 Ultrasonic Sensors (US) dislocated along the channel. Some differences in wave behaviour and structure were observed between all tested scenarios. As expected, the surge propagating on a rough bed had lower velocities, whereas similar height profiles and velocities were observed for the bores propagating over an initial still water depth of 5 cm, suggesting that the bed roughness had less or almost no influence. All test cases were conducted with a high Reynolds number ($Re \approx 10^7$), implying a highly turbulent flow. The regular and less oscillating pattern observed for the rough configurations suggested a higher level of internal smaller-scale turbulence, which was able to more efficiently dissipate larger eddies, whereas in the smooth configuration the residual energy was dissipated with repetitive surface fluctuations.

A frequency domain analysis was carried out and through FFT power spectra of the wave height profiles were obtained for all configurations. A Reynolds-like decomposition was applied to the wave height signal, allowing to isolate the fluctuations of the surface turbulence. A difference in the shape of the spectra was observed between the increasing (head) and the decreasing (tail) parts of the wave from the wave profile. The head was characterised by higher frequencies compared to the tail, with larger amplitude. The computation of the integral of the spectrum showed higher energy associated to the tail for frequencies between 0.5 and 6 Hz.

As the surface turbulence of propagating waves is random and highly 3-dimensional, an accurate reproduction at laboratory scale can be challenging. The turbulent behaviour of the surface secondary waves could represent a mean to verify the flow pattern repeatability of the hydrodynamic behaviour behind the bore front. The study proposes a simple methodology to evaluate free-surface oscillations and its energy content associated with dominant frequencies, however it was applied only to a limited number of transient wave signals. Future work should consider a larger set of signals and include an analysis of the data set cumulative duration as a mean to characterise the ensemble turbulent energy content of such transient waves.

NOTATION

d_0	Equivalent impoundment depth [m]	$h_{m.av}$	Height profile moving average [h]
D_H	Hydraulic diameter [m]	P_{xx}	Spectral density [m^2/Hz]
f	Darcy-Weisbach friction factor [-]	R	Hydraulic radius [m]
F	Frequency [Hz]	Re	Flow Reynolds number [-]
Fr	Flow Froude Number [-]	t	Time [s]
Fr_B	Bore Froude Number [-]	U	Wave front velocity [m/s]
g	Gravitational constant [m/s^2]	x	Channel distance [m]
h	Wave height [m]	σ^2	Wave height Variance [m^2]
h'	Wave fluctuation [m]	v	Kinematic viscosity [m^2/s]
h_0	Initial still water depth [h]		

ACKNOWLEDGEMENT

The support of the Swiss National Science Foundation (SNSF), grant 200021_149112 /1, is acknowledged.

REFERENCES

Arnason H., Petroff C., and Yeh H. (2009). Tsunami bore impingement onto a vertical column. *Journal of Disaster Research*, 4, 6, 391–403.

Chanson H. (2010). Unsteady turbulence in tidal bores: effects of bed roughness. *Journal of Waterway, Port, Coastal, and Ocean Engineering*.

Chanson H., Aoki S., and Maruyama M. (2002). Unsteady air bubble entrainment and detrainment at a plunging breaker: dominant time scales and similarity of water level variations. *Coastal Engineering*, 46, 2, 139–157.

Choufi L., Kettab A. and Schleiss A.J. (2014). Effet de la rugosité du fond d'un réservoir rectangulaire à faible profondeur sur le champ d'écoulement. *La Houille Blanche*, 5, 83-92.

Chow V.T. (1959). Open channel hydraulics. *McGraw-Hill*, New York, USA.

Cross R. (1967). Tsunami surge forces. *Journal of the Waterways and Harbours Division*, 93, 4, 201–231.

Chanson H. and Docherty, N. J. (2012). Turbulent velocity measurements in open channel bores. *European Journal of Mechanics B/Fluids*, 32, 52-58.

Favre H., 1935. Etude théorique et expérimentale des ondes de translation dans les canaux découverts. *Dunod*, Paris.

Henderson F. M. (1966). Open channel flow, Macmillan, New York

Koch C. and Chanson H. (2009). Turbulence measurements in positive surges and bores. *Journal of Hydraulic Research*, 47, 1, 29-40

Kolmogorov A. (1931). Über die analytischen Methoden in der Wahrscheinlichkeitsrechnung (On analytical methods in the theory of probability). *Mathematische Annalen*, 104.

Leng X. and Chanson H. (2015). Breaking bore: Physical observations of roller characteristics. *Mechanics Research Communications*, 65, 24-29

Longuet-Higgins M.S. and Turner J.S. (1974). An 'entraining plume' model of a spilling breaker. *Journal of Fluid Mechanics*, 63, 1, 1-20.

Marche C., Beauchemin P., & El Kayloubi A., 1995. Étude numérique et expérimentale des ondes secondaires de Favre consécutives à la rupture d'un barrage, *Canadian Journal of Civil Engineering*, 22, 4, 793-801.

Meile T. (2007). Influence of macro-roughness of walls on steady and unsteady flow in a channel. *Ph.D. Thesis N.3952*, EPFL-LCH, Lausanne Switzerland, 414 pages and Vol. 36 of Communication of Laboratory of Hydraulic Constructions (LCH), EPFL, Ed. A-Schleiss. ISSN 1661-1179

Meile T., Boillat J.L., & Schleiss A.J., 2013. Propagation of surge waves in channels with large-scale bank roughness, *Journal of Hydraulic Research*, 51, 2, 195-202.

Nistor I., Palermo D., Nouri Y., Murty T., and Saatcioglu M. (2009). Tsunami-induced forces on structures. *Handbook of Coastal and Ocean Engineering. Singapore,* World Scientific, 261–286.

Ramsden J. (1993). Tsunami-forces on a vertical wall caused by long waves, bores and surges on a dry bed. *PhD Thesis. California Institute of Technology*, Pasadena, California, 218 pages.

Reungoat D., Chanson H., and Keevil C. (2015). Field Measurements of Unsteady Turbulence in a Tidal Bore: the Garonne River in October 2013. *Journal of Hydraulic Research*, 10, 291-301

Ritter A. (1892). Die fortpflanzung de wasserwellen. *Zeitschrift Verein Deutscher Ingenieure*, 36, 33, 947-954

Rossetto T., Allsop W., Charvet I., and Robinson D. (2011). Physical modelling of tsunami using a new pneumatic wave generator. *Coastal Engineering*, 58, 6, 517–527.

Soares Frazao S., & Zech Y. (2002). Undular bores and secondary waves-experiments and hybrid finite-volume modelling. *Journal of Hydraulic Research*, 40, 1, 33-43.

Stoker J. J. (1957). Waler Waves: The Mathematical Theory with Applications. *Intersciences*, 567 pages

Terrier S., Bieri M., De Cesare G. and Schleiss A.J. (2014). Surge Wave Propagation in a Common Tailrace Channel for Two Large Pumped-Storage Plants. Journal of Hydraulic Engineering, 140, 218-225

Wilson J., Gupta R., Van de Lindt J., Clauson M., and Garcia R. (2009). Behavior of a one-sixth scale wood-framed residential structure under wave loading. *Journal of Performance of Constructed Facilities*, 23, 5, 336–345.

Wüthrich D., Nistor I., Pfister M. and Schleiss A.J. (2016). Experimental generation of tsunami-like waves. *Proceedings of Coastal Structures*. Boston, MA, USA. 9-11 September.

Yeh H. and Mok K.M. (1990). On turbulence in bores. *Physics of Fluids A: Fluid Dynamics (1989-1993)*, 2, 5, 821-828.

Yeh H., Ghazali, A., and Marton, I. (1989). Experimental study of bore run-up. *Journal of fluid Mechanics*, 206, 563–578.